Origin of *p*-type conduction in single-crystal CuAlO$_2$

J. Tate,[1,*] H. L. Ju,[2,†] J. C. Moon,[2] A. Zakutayev,[1] A. P. Richard,[3] J. Russell,[1] and D. H. McIntyre[1]

[1]*Department of Physics, Oregon State University, Corvallis, Oregon 97330, USA*
[2]*Department of Physics, Yonsei University, Seoul 120-749, Korea*
[3]*Department of Chemistry, Oregon State University, Corvallis, Oregon 97330, USA*

We report measurements of the structural, optical, transport, and magnetic properties of single crystals of the anisotropic *p*-type transparent semiconductor CuAlO$_2$. The indirect and direct band gaps are 2.97 and 3.47 eV, respectively. Temperature-dependent Hall measurements yield a positive Hall coefficient in the measured range and an activated carrier temperature dependence. The resistivity is anisotropic, with the *ab*-plane resistivity about 25 times smaller than the *c*-axis resistivity at room temperature. Both are activated with similar activation energies. The room-temperature *ab*-plane mobility is relatively large at 3 cm^2 V^{-1} s^{-1}, and we infer a *c*-axis mobility of 0.12 cm^2 V^{-1} s^{-1}. The Seebeck coefficient is positive at all measured temperatures, and has a T^{-1} dependence over most of the measured range. The low-temperature paramagnetic moment is consistent with a spin-1/2 defect with a density of 3.4×10^{20} cm^{-3}. These results suggest that the conduction mechanism for *p*-type carriers in CuAlO$_2$ is charge transport in the valence band and that the holes are thermally activated from copper-vacancy acceptor states located about 700 meV above the valence-band maximum.

I. INTRODUCTION

CuAlO$_2$ belongs to the delafossite family of oxides with general formula Cu*M*O$_2$, where *M* includes Fe, Co, Rh, Al, Ga, In, Sc, Y, or a lanthanide.[1,2] This class of materials has been studied extensively since CuAlO$_2$ was reported as a transparent *p*-type conductor in thin-film form.[3] The promise of applications in transparent electronics triggered a flurry of efforts to produce thin-film *p*-type wide-gap semiconductors to complement the existing wide-gap *n*-type semiconductors such as ZnO, SnO$_2$, and In$_2$O$_3$. There have been comparatively few studies of the single-crystal form of the delafossites. Such studies should reveal the intrinsic properties and elucidate transport mechanisms and fundamental optical and magnetic properties. In particular, with few exceptions, mobilities reported for Cu*M*O$_2$ thin films are less than 1 cm^2 V^{-1} s^{-1}, and no mobility measurements are available for single crystals, so it is not known whether the material limits have been reached.

The Cu*M*O$_2$ structure (Fig. 1) comprises alternating Cu^{1+} layers (*ab* plane) and corner-sharing *M*O$_6$ octahedra stacked along the *c* axis. Each Cu^{1+} ion is twofold coordinated by oxygen, forming a dumbbell structure that connects the *M*O$_6$ octahedra.[4] The layered structure decreases Cu-Cu interactions and increases the band gap relative to Cu$_2$O, which is also a *p*-type semiconductor, but is isotropic and has E_g =2.1 eV. This anisotropic geometrical arrangement of the atoms should give rise to anisotropic transport and optical properties.[1,5] The Cu^{1+} layers are expected to be the main conduction channel, with more limited conductivity perpendicular to the layers. Anisotropic transport properties of the Cu*M*O$_2$ oxides have not been well established, except for the early reports of Shannon *et al.*[5] (which did not include CuAlO$_2$) and the more recent reports of Lee *et al.*[6] and Koumoto *et al.*[7] None of these reports included mobility measurements.

The electrical-conduction mechanisms of CuAlO$_2$ are still controversial, and CuAlO$_2$ has been reported to exhibit variable-range hopping,[6] band-conduction,[3,8] and small polaron transport.[9] Since most reported experiments were performed on thin film and bulk materials, these results are likely to be influenced by grain boundaries, strain and other defects common in such materials. Such defects limit carrier mobility, and single-crystal measurements should measure the intrinsic carrier mobility, and determine whether true band conductivity is possible.

In addition, the origin of *p*-type carriers in nominally undoped CuAlO$_2$ has not been clarified. The conductivity in nominally undoped Cu*M*O$_2$ is invariably *p* type, small, and increases strongly with increasing temperature. Evidently the materials are prone to spontaneously producing acceptorlike defects that reside within the gap. Raebiger *et al.*[10] and Nolan[11] have calculated defect formation energies in CuAlO$_2$ and related materials and concluded that Cu vacancies are the most likely defect. Ingram *et al.*[12] have proposed a Cu/Al complex as the relevant defect to explain the conductivity at high temperature.

In this study of CuAlO$_2$ single crystals, we report a fairly large *ab*-plane room-temperature hole mobility (3.0 cm^2 V^{-1} s^{-1}) and a resistivity anisotropy of 40–25 in the temperature range 180–350 K. The carrier-density temperature dependence is consistent with band conductivity resulting from the ionization of a defect, probably a Cu vacancy, that lies about 700 meV above the valence band. There is a low-temperature paramagnetic moment consistent with a density of about 10^{20} cm^{-3} spins that may be related to this defect.

II. EXPERIMENT

Crystals of CuAlO$_2$ were grown by a method similar to that described by Ishiguro *et al.*[13] CuAlO$_2$ powder was made according to the reaction
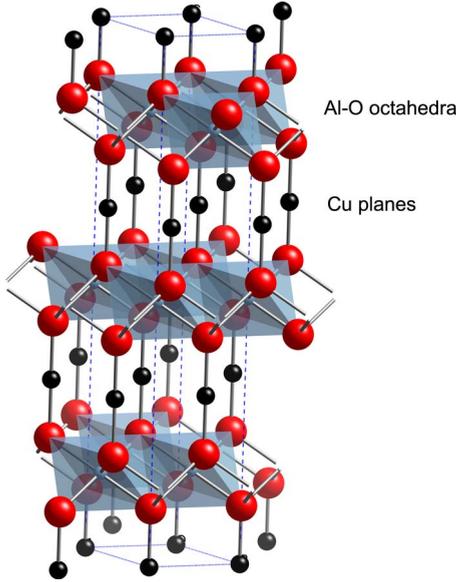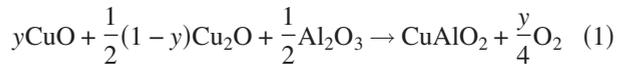
FIG. 1. (Color online) The crystal structure of the 3R polytype of CuAlO$_2$. Alternating layers of Cu atoms and AlO$_6$ octahedra stacked along the c axis give the structure its anisotropic character.

$$yCuO + \frac{1}{2}(1-y)Cu_2O + \frac{1}{2}Al_2O_3 \rightarrow CuAlO_2 + \frac{y}{4}O_2 \quad (1)$$

with y in the range 0.4–0.6. Powders of CuO, Cu$_2$O, and Al$_2$O$_3$ (200 mesh) were mixed in stoichiometric proportions, finely ground, and heated to 1100 °C for 5 days in air. The resulting powder was a mixture of CuAlO$_2$ and CuO. Approximately 5 g of this powder was added to 40 g of CuO powder to almost fill a 30 mL alumina crucible, which was covered with soft refractory brick, placed inside an electrical furnace, and heated to 1200 °C. After 5 h at 1200 °C, the system was cooled at a rate of 5 °C/h to 1050 °C, and then at 300 °C/h to room temperature. CuAlO$_2$ crystals were separated from the matrix by leaching in hot 1M HNO$_3$ for 3 days. Additional washing with 1M H$_3$NSO$_3$ reduced any residual CuO flux still further. The unit-cell parameters were examined by a single-crystal Bruker Apex CCD x-ray diffractometer with Mo $K\alpha$ radiation (0.71073 Å). Smaller crystals were reground into powder and conventional x-ray powder analysis was performed with Cu K radiation.

The CuAlO$_2$ crystals for optical and transport measurements were polished to reduce both surface roughness and thickness. The dimensions of the single crystals were measured with an optical microscope. Low-resistance, Ohmic contacts are critical for transport measurements and for the accurate determination of activation energies and anisotropy parameters. Vacuum-evaporated, 200-nm-thick Au contact electrodes were defined with metal shadow masks, and thermally annealed in rough vacuum (1 mtorr) at 400 °C for 30 min to reduce contact resistance. Then, 50-μm-diameter Au wires were attached to the contact electrodes with silver epoxy. The transport results presented in Figs. 3 and 4 were reproducible using several different contact pairs and many different crystals (for *ab*-plane measurements), and using several crystals polished to different thicknesses (for *c*-axis

measurements). The contacts were Ohmic, and typical contact resistance values at room temperature were less than 2% of the sample resistance for *ab*-plane measurements and less than 10% for *c*-axis measurements.

The *ab*-plane resistivity (ρ_{ab}) and *c*-axis resistivity (ρ_c) of CuAlO$_2$ single crystals were measured from 180–350 K in a Quantum Design Physical Property Measurement System (PPMS) by a four-terminal-four-probe and a two-terminal-four-probe technique, respectively, illustrated in the insets to Fig. 4. Hall measurements in the *ab* plane were carried out in a LakeShore 7504 Hall Measurement System, in a magnetic field of 1.5 T in the temperature range 290–430 K. Small circular Au contacts (0.03 mm^2) were deposited on the periphery of the large, flat face of the crystal in the van der Pauw configuration illustrated in the inset to Fig. 3(c).

The Seebeck coefficients of ~50-μm-thick CuAlO$_2$ single crystals, mounted on Al$_2$O$_3$ substrates, were measured from 90–300 K in a home-built system based on a closed-cycle He refrigerator. The temperature gradient was measured with a chromel/alumel/chromel differential thermocouple attached to the crystal with an electrically insulating epoxy, and the voltage difference was measured with Au leads attached to Ohmic Au contacts with electrically conducting silver epoxy. The small size of the crystal made it difficult to determine the temperature gradient with good precision, so we consider the Seebeck measurements to be good qualitative trend indicators, but less quantitatively reliable than resistivity and Hall measurements in determining materials parameters.

Optical transmission measurements in the range 200–2600 nm were made on polished 20-μm-thick single crystals with the light beam incident along the c axis. The diameter of the beam spot was about 1.5 mm. The spectrometer is based on an Ocean Optics HR 4000 uv-visible spectrometer (200–1100 nm, resolution 0.27 nm) with a balanced deuterium/tungsten halogen source and an Ocean Optics NIR256–2.5 near-infrared spectrometer (800–2600 nm, resolution 6.85 nm) with a tungsten halogen source. In each spectrometer, broadband light is incident on the sample via a fiber optic, and collected after transmission in a second fiber optic, which delivers the transmitted light to a grating where it is dispersed and detected on a linear charge-coupled device array (uv visible) or photodiode array (near infrared).

Dc magnetic-susceptibility measurements on many crystals, totaling 180 mg, were carried out with a Quantum Design PPMS in a magnetic field of 5000 Oe in the temperature range 5–300 K. Care was taken to avoid magnetic contaminants by careful handling of the crystals with nonmetal tools. Similar measurements were made on independently prepared CuAlO$_2$ powder. The dc magnetic susceptibility of CuO powder was also measured in the same temperature range so as to estimate the effect of any residual CuO flux on the CuAlO$_2$ susceptibility.

III. RESULTS

A. Structure

A typical CuAlO$_2$ crystal grown from the CuAlO$_2$/CuO flux was dark blue, lustrous and platelike in shape. The
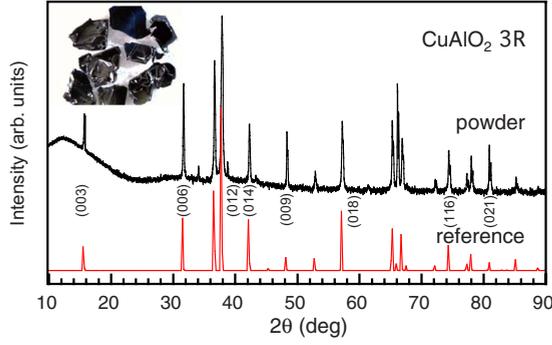
FIG. 2. (Color online) Powder x-ray diffraction pattern of CuAlO$_2$ (upper trace, logarithmic scale). The powder was made from grinding single crystals similar to those depicted in the inset. The lower trace (linear scale) is the reference pattern for the 3R polytype.

ab-plane dimensions of 1–2 mm, and a thickness of about 100–200 μm. Single-crystal x-ray diffraction revealed that the crystals contain no impurity phases, and have a hexagonal unit cell with $a=b=2.857(2)$ Å, $c=16.959(7)$ Å, and $V=119.87(1)$ Å^3.

These cell dimensions match the parameters for the 3R polytype. The c axis is perpendicular to the flat face of the crystal, which makes it relatively easy to separate the *ab*-plane and *c*-axis transport properties. The x-ray diffraction pattern of smaller crystals ground into a powder is displayed in Fig. 2. All peaks between $10°-90°$ 2θ are less than $0.1°$ in 2θ and can be indexed to 3R CuAlO$_2$ with $a=b=2.855$ Å, $c=16.958$ Å. All peaks display $K\alpha_1$ and $K\alpha_2$ doublets, which can be easily resolved at large 2θ, and the $K\beta$ peak of the most intense reflection (012) is also visible. The (00l) peaks appear with a larger intensity than predicted from a powder sample because the crystallites are platelike and tend to align. There may be some evidence of the most intense peak of 2H CuAlO$_2$, but it overlaps the 3R (012) peak. There is one very small peak at $2\theta \approx 38.8°$ that is consistent with the $K\alpha$ reflection from one of the two most intense CuO lines. We conclude that the single crystals are phase pure and of very good quality, but that a very small residue of the CuO flux may remain on the surface. We subsequently reduced the CuO residual with an acid wash, and found no significant change in the magnetic susceptibility of CuAlO$_2$.

B. Transport properties

Figure 3 shows the results of the Hall measurements, the carrier density p, the *ab*-plane resistivity ρ_{ab}, and the mobility μ_{ab} of one of the CuAlO$_2$ crystals. Reliable and reproducible results with low contact resistance were limited to the relatively high-temperature range ($290 < T < 430$ K). The Hall coefficient R_H was positive at all temperatures, confirming *p*-type conduction, and the value at 300 K was $+47$ cm^3 C^{-1}. The carrier density was calculated from the Hall coefficient assuming single band conduction, i.e., $p=1/qR_H$. The carrier density [Fig. 3(a)] increased by a factor of 100 from 7.8×10^{16} cm^{-3} at 290 K to 8.1×10^{18} cm^{-3} at
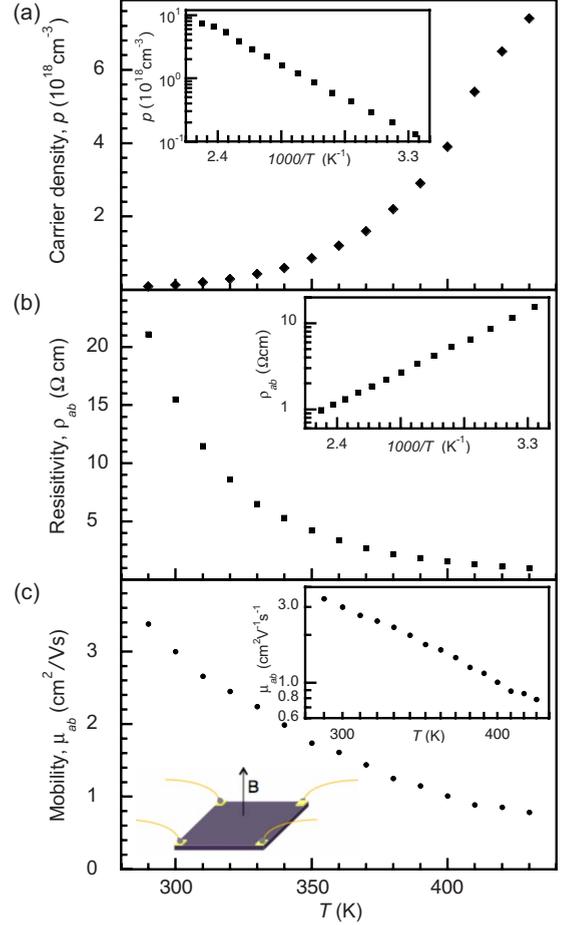

FIG. 3. (Color online) Temperature-dependent transport properties of single-crystal CuAlO$_2$ measured in the *ab* plane. (a) The hole carrier density p determined from in-plane Hall coefficient measurements. (b) The in-plane resistivity ρ_{ab}. (c) The mobility μ derived from ρ_{ab} and p. Insets show the linearity of log p and log ρ_{ab} vs $1/T$, and of log μ vs log T, and the van der Pauw contact configuration.

430 K. If a model of thermal activation of carriers from defect to band states is correct, then the carrier density is

$$p = p_0 e^{-U/k_B T}, \qquad (2)$$

where p_0 is a prefactor and U is an activation energy related to the position of the acceptor level relative to the valence-band edge, which will be discussed further in Sec. IV. The inset to Fig. 3(a) illustrates the linearity of log p vs $1/T$ and the slope of the line yields $U=350$ meV. Such linearity suggests thermal activation of the holes from defect to band states, and subsequent band conduction.

Figure 3(b) shows, for the same crystal, the semiconductorlike temperature dependence of the *ab*-plane resistivity ρ_{ab}, which decreases by a factor of 20 from 20 Ω cm at 290 K to 1 Ω cm at 430 K. Figure 4(a) shows ρ_{ab} for a different crystal measured in a different system in the temperature range 180–350 K. The data agree very well in the region of overlap. Figure 4(a) also shows the *c*-axis resistivity ρ_c, which is higher than ρ_{ab} by a factor of 25 at room tempera-
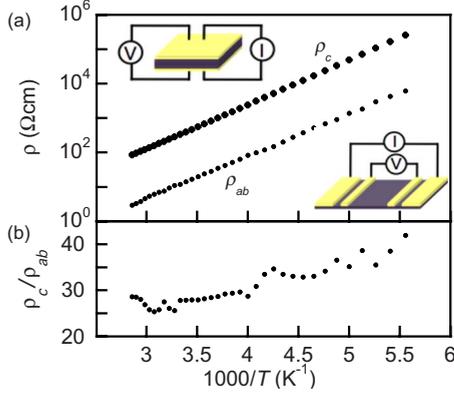
FIG. 4. (Color online) (a) Resistivity of a single crystal of CuAlO$_2$ from 180 to 290 K measured in the *ab* plane and in the *c*-axis direction. The insets show the contact configuration. (b) The temperature-dependent resistivity anisotropy.

FIG. 5. Seebeck coefficient of a CuAlO$_2$ single crystal. The sharp increase at low temperatures is indicative of semiconducting behavior. Inset: power factor $S^2\sigma$. The data for $T < 400$ K are from this work, while the higher temperature data are from Ref. 7.

ture and a factor of 40 at 180 K. The resistivity anisotropy is plotted in Fig. 4(b).

The resistivity data also appear linear on a log ρ vs $1/T$ plot [inset to Fig. 3(b)]. In a band-conduction model, the resistivity is related to the carrier density p and the carrier mobility μ and the fundamental charge q via

$$\rho = (pq\mu)^{-1} \tag{3}$$

which leads to an Arrhenius-type behavior

$$\rho = \rho_0(T)e^{U/k_BT}, \tag{4}$$

but the prefactor contains the mobility, whose temperature dependence may be significant. Nevertheless, if we ignore this prefactor temperature dependence, we obtain U =236 meV from the higher temperature ρ_{ab} data in Fig. 3(b), and U=243 meV from the ρ_{ab} data and U=256 meV from the ρ_c data in Fig. 4(a). These values are internally consistent, but significantly smaller than the value U=350 meV extracted from the carrier-density data, which indicates that temperature dependence of the prefactor in Eq. (4) is not sufficiently weak to ignore.

The mobility in the *ab* plane was calculated from the resistivity and carrier concentration according to Eq. (3), and is displayed in Fig. 3(c). The mobility at 300 K is 3.0 cm^2 V^{-1} s^{-1}, well above values predicted for polaron conduction (<1 cm^2 V^{-1} s^{-1}) (Ref. 9) and larger than most reported mobility values for CuAlO$_2$, which are less than 1 cm^2 V^{-1} s^{-1} (Refs. 14 and 15) except for the thin-film results of Kawazoe *et al.* (10.4 cm^2 V^{-1} s^{-1}),[3] and Lan *et al.* (4.07 cm^2 V^{-1} s^{-1}).[16] This suggests that our crystal quality is very good and that we may be measuring intrinsic mobility that is not limited by defects. As the temperature increases, the mobility decreases from 3.4 cm^2 V^{-1} s^{-1} at 290 K to 0.8 cm^2 V^{-1} s^{-1} at 430 K.

The *c*-axis mobility μ_c could not be directly measured because the crystals were too thin for reliable Hall measurements to be made in the *c* direction, but it can be inferred from knowledge of the mobility and anisotropy at room temperature. The resistivity anisotropy $\frac{\rho_c}{\rho_{ab}}$ [Fig. 4(b)] is effec-
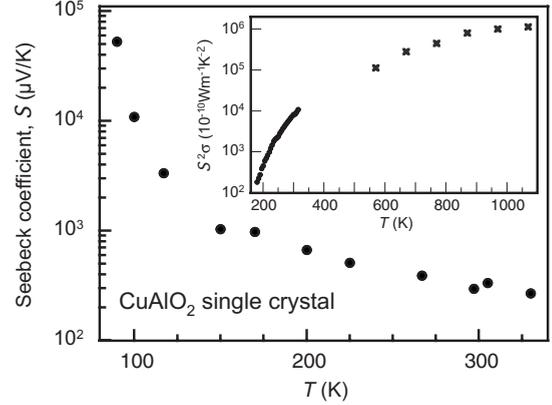
tively a mobility anisotropy $\frac{\mu_{ab}}{\mu_c}$ because p is independent of the carrier transport direction. At room temperature μ_c =0.12 cm^2 V^{-1} s^{-1}. Thus the data indicate that both μ_{ab} and μ_c increase with decreasing temperature, but that μ_c increases somewhat more slowly. The difference could be due to a different phonon distribution in the two directions, or to larger disorder in the *c* direction from stacking faults of the 2H and 3R polytypes. The temperature dependence of the *ab*-plane mobility in Fig. 3(c) is not the textbook $\mu \propto T^{-3/2}$ dependence expected from acoustic phonon scattering,[17] but rather stronger, $\mu \propto T^{-3.8}$ [inset to Fig. 3(c)], for which there is no readily obvious mechanism. We know of no mechanism that would cause such strong temperature dependence, but a T^{-3} mobility dependence has been observed in the "infinite layer" Sr$_{1-x}$Cu$_2$O materials.[18] It is possible to fit the $\mu_{ab}(T)$ data to a polaron-type dependence where the mobility would be exponentially activated because of carrier trapping by the distortion of the lattice by polar optical phonons.[9] Such a fit yields an activation energy of 10 meV, which seems too small to be characteristic of optical phonons, which are several tens of meV.[19,20] The T^{-1} temperature dependence of the Seebeck coefficient discussed below also seems to support a more conventional band mechanism.

The Seebeck coefficient S and power factor $S^2\sigma$, where $\sigma = 1/\rho$ is the conductivity, of a CuAlO$_2$ single crystal between 90 and 330 K are shown in Fig. 5. The S and ρ data for $T < 400$ K are from this work, while the higher temperature data are from Koumoto *et al.*[7] The sign of thermopower of CuAlO$_2$ is positive, confirming the Hall result. The magnitude at room temperature ($\sim$300 μV K^{-1}) is fairly large, indicative of semiconducting behavior. With decreasing temperature, S increases approximately as T^{-1} for $T > 150$ K indicating thermally activated behavior from an acceptor state to the valence band and then increases much faster than T^{-1} for $T < 150$ K. This faster increase may be a phonon drag effect. The temperature dependence of S is clearly different from the $T^{1/2}$ dependence suggested for a variable range hopping model[21] and also different from the constant value predicted by a small polaron model.[9]

The Seebeck data qualitatively support the transport mechanism suggested by the resistivity results. For a semi-
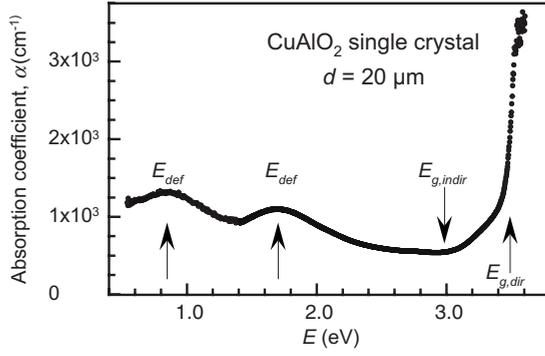
FIG. 6. Optical absorption at room temperature of a 20 μm-thick CuAlO$_2$ single crystal with light incident along the c axis. Two defect absorptions at 0.85 and 1.75 eV are evident. At higher energies band-to-band absorption occurs, with an indirect gap at 2.97 eV and a direct gap at 3.47 eV. The absorption values are systematically high because reflection from the faces of the crystal is not accounted for.

conductor exhibiting band conduction, the Seebeck coefficient is

$$S = \frac{k_B}{e} \left[\ln\left(\frac{N_V}{p}\right) + \frac{5}{2} + r \right], \quad (5)$$

where N_V is the effective density of states at the valence-band maximum, p the mobile hole density, and k_B and e are Boltzmann's constant and the fundamental charge. The constant r is defined by the energy dependence of the mean scattering time $\tau \approx E^r$.[17] With

$$p = N_V e^{-(E_F - E_V)/k_B T}, \quad (6)$$

where $E_F - E_V$ is the difference between the Fermi energy and the valence-band maximum, this yields

$$S = \frac{k_B}{e} \left(\frac{E_F - E_V}{k_B T} + \frac{5}{2} + r \right) \propto \frac{1}{T} + \text{const.} \quad (7)$$

For temperatures $T > 150$ K, a fit to Eq. (7) yields $E_F - E_V$ in the range 260–350 meV depending on the exact temperature interval used. This value is in reasonable agreement with other measures of the defect energy level as we discuss in Sec. IV.

C. Optical and magnetic properties

The optical absorption, α, of a 20-μm-thick CuAlO$_2$ crystal is displayed in Fig. 6. The absorption is calculated from the transmission without correction for surface reflection. We associate the dominant feature of a large change in absorption near 3.5 eV with absorption across a direct gap, and the more subtle increase starting near 3.0 eV with absorption across the indirect gap. More quantitative analysis, namely, plotting $(\alpha E)^n$ vs photon energy E, with $n = \frac{1}{2}$ for an indirect gap and $n = 2$ for a direct gap and extrapolating the linear portion to the energy intercept on the $\alpha = 0$ axis, yields gap values of $E_{g,d} = 3.47$ eV and $E_{g,i} = 2.97$ eV, in good agreement with other experimental results on single crystals.[22] The indirect gap is larger than reported for thin films, and may
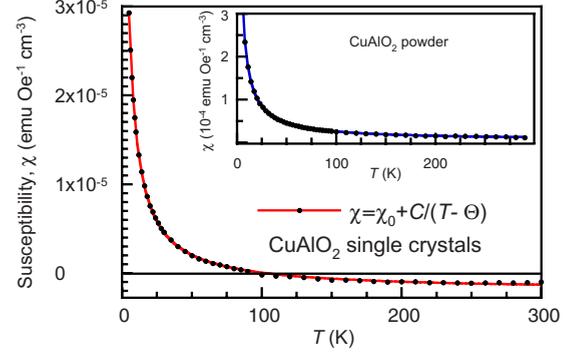

FIG. 7. (Color online) Magnetic susceptibility of 186 mg of CuAlO$_2$ single crystals from 5 to 300 K. Inset: magnetic susceptibility of CuAlO$_2$ powder.

indicate that the thin-film results are dominated by strain effects. Other features in the optical spectrum are broad absorptions at $E = 1.7$ and 0.85 eV, which we discuss further in Sec. IV.

The magnetic susceptibility of a collection of CuAlO$_2$ single crystals was measured from 5 to 300 K in 5 K steps in an applied external magnetic field of 5000 Oe. The temperature dependence of the magnetic susceptibility is shown in Fig. 7. The susceptibility data can be fit with the Curie-Weiss formula

$$\chi = \chi_0 + \frac{C}{T - \Theta}, \quad (8)$$

where χ_0, Θ, and C are the temperature-independent susceptibility, the Curie-Weiss temperature, and Curie constant, respectively.[23] The best-fit values to χ_0, Θ, and C are $-2.00(2) \times 10^{-6}$ emu cm^{-3} Oe^{-1}, $-1.67(5)$ K, and $2.09(1) \times 10^{-4}$ K, respectively. The Curie constant can be expressed as

$$C = \frac{N g^2 \mu_B^2 S(S+1)}{3k_B}, \quad (9)$$

where N is the number density of the magnetic ions, g is the Landé g factor, S is the magnitude of the electron spin (not to be confused with the earlier use of S for the Seebeck coefficient), and μ_B is the Bohr magneton.[23] Assuming that the magnetic moment arises from a defect state with $S = 1/2$, the estimated density of paramagnetic defects is $N = 3.4 \times 10^{20}$ cm^{-3}. In fully stoichiometric CuAlO$_2$, free of magnetic impurities, only Cu^{1+}, Al^{3+}, and O^{2-} species exist, none of which have unpaired electrons and thus there should be no paramagnetism. However, as we discuss in Sec. IV, the literature indicates that nonstoichiometry in the form of Cu vacancies (V_{Cu}) is likely. Whether such vacancies produce a localized spin-1/2 species, and hence paramagnetism, remains an open question. However, it is interesting to note that the value of N is about 1.3% of the density (2.5×10^{22} cm^{-3}) of Cu sites in CuAlO$_2$ and electron-probe microanalysis (EPMA) indicates that the crystal stoichiometry has a Cu deficiency of $5 \pm 4\%$.

The temperature-independent susceptibility has contributions from core diamagnetism and paramagnetism due to

conduction charges and crystal-field energy-level splitting. Since CuAlO$_2$ is a wide-gap semiconductor, the number of conduction electrons/holes is small, we ignore any paramagnetic contribution from conduction charges. The lack of knowledge about crystal-field energy-level splitting forces us to assume that paramagnetic contribution from crystal-field splitting is small and can be ignored. Thus χ_0 is approximately equal to χ^{core}. A value of -1.58×10^{-6} emu cm^{-3} Oe^{-1} for the core diamagnetic susceptibility χ^{core} estimated from tabulated values for Cu^{1+}, Al^{3+}, and O^{2-} (Ref. [24]) is within 20% of the value -2.0×10^{-6} emu cm^{-3} Oe^{-1} obtained from the fit to Eq. (8). More careful measurements in the low-temperature regime would be required to ascertain whether there is any physical significance to the small negative value of Θ in the fit.

The question of residual paramagnetic contribution from residual CuO flux must be addressed. Very small quantities of CuO flux present on the surface of the crystals would not affect transport results on single crystals, but the magnetic-susceptibility measurement required several hundred single crystals and a signal from residual flux might be significant. CuO is antiferromagnetic with a Neel temperature of 220 K,[25] so, in principle, it should not contribute to low-temperature paramagnetism, and indeed some authors have reported a small, temperature-independent susceptibility well below the Neel temperature.[26] In contrast, others have reported a paramagnetic contribution to the low-temperature single-crystal CuO susceptibility, suggested to be from noncoupled spins at a density of 10^{21} cm^{-3}.[27] We measured the susceptibility of about 200 mg of the CuO powder used for the flux, and found a low-temperature paramagnetic signal consistent with unpaired spins at a density of about 10^{20} cm^{-3}. Because the magnetic signal is proportional to the total number of spins, and the CuO contributes considerably less than 1% to the x-ray diffraction signal, we can conclude that the magnetic susceptibility measured for the CuAlO$_2$ crystals is in error by at most 1% due to the presence of residual CuO flux. We also note that we have measured a similar low-temperature paramagnetic moment in CuAlO$_2$ powders, as shown in the inset to Fig. 7. These powders were prepared independently by a conventional solid-state synthesis that did not involve excess CuO flux.

IV. DISCUSSION

The structural, transport, and optical properties of single-crystal CuAlO$_2$ reported in the previous section provide a coherent picture of the *p*-type conduction mechanism and the origin of *p*-type carriers. We suggest that the measurements are consistent with band conduction of holes that are generated from an acceptor level located about 700 meV above the top of the valence band. This acceptor level is likely to be generated by copper vacancies.

The mechanism of conduction in CuAlO$_2$ has been reported to be of the small polaron type in pressed pellets at temperatures above 900 K,[9] based on an activated conductivity and a temperature-independent Seebeck coefficient (thermopower). Ingram *et al.*[9] conclude that the mobility of their CuAlO$_2$ powders is less than 0.1 cm^2 V^{-1} s^{-1}, which is
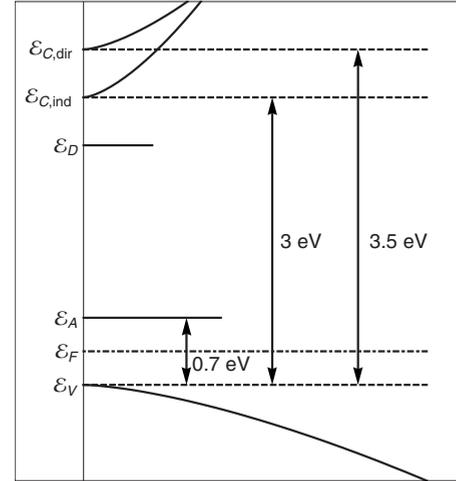

FIG. 8. Energy-level diagram showing acceptor levels about 700 meV above the valence-band maximum. The donor density is much lower than the acceptor density, and the Fermi level is approximately half way between ε_A and the valence-band maximum. Direct and indirect band gaps are 3.47 and 2.97 eV, respectively.

reasonable for a polaron model. Lan *et al.*[16] reported two-dimensional variable-range hopping ($\log \rho \propto T^{-1/3}$) at temperatures lower than 180 K in high-quality CuAlO$_2$ thin films, with a crossover to conventional activated conductivity ($\log \rho \propto T^{-1}$) at higher temperatures. The room-temperature mobility of their films, 4.0 cm^2 V^{-1} s^{-1}, is one of the highest reported for CuAlO$_2$ in any form. The report of 10.4 cm^2 V^{-1} s^{-1} at room temperature in the original report of *p*-type CuAlO$_2$ thin films has not been reproduced.

Our conductivity and Seebeck results from single-crystal CuAlO$_2$ span the intermediate temperature range 180–430 K, and, coupled with the magnetic and optical data, can be interpreted reasonably consistently in terms of a band-conduction model with acceptors located about 700 meV above the valence-band supplying holes for conduction. The Seebeck and Hall measurements confirm *p*-type conduction of CuAlO$_2$. The room-temperature mobility of 3.0 cm^2 V^{-1} s^{-1} in CuAlO$_2$ single crystals is reproducible and robust, and this relatively large value indicates that a polaron model of conductivity is unlikely in this temperature range, since polaron mobilities are generally considered to be below 1 cm^2 V^{-1} s^{-1}. As demonstrated in the previous section, the carrier density obeys an Arrhenius behavior of Eq. (2), with an activation energy of $U = 350$ meV. Clearly the temperature ranges considered here are too low for intrinsic conductivity to be important (the band gap is about 3 eV $\approx 3.6 \times 10^5$ K), therefore defect levels determine the carrier concentration, and U is related to the defect binding energy. The particular relationship between U and the defect binding energy ε_A depends on the temperature range. Consider the simplest case of a single acceptor level of density N_A and binding energy ε_A and a single donor level of density N_D and binding energy ε_D, as shown in Fig. 8. If the defect levels were fully ionized, then there would be no dependence of the carrier density on temperature. So assuming that $N_A > N_D$, and that the hole density p is much greater than the electron density n, it is readily shown for a nondegenerate semiconductor that the hole density is given by[28]

$$p + N_D = \frac{N_A}{1 + \frac{\gamma p}{N_V} e^{\varepsilon_A / k_B T}}, \tag{10}$$

where $N_V = 2(2 m_V^* k_B T / \hbar^2)^{3/2}$ is the effective density of states at the valence-band maximum determined by the hole effective mass m_V^*, and γ is a degeneracy factor that is greater than one for an acceptor defect. Solving for p in a temperature range where $p \gg N_D$ (i.e., compensation by the donor defects has little effect on the carrier concentration), we find

$$p = \left(\frac{N_A N_V}{\gamma} \right)^{1/2} e^{-\varepsilon_A / 2 k_B T}. \tag{11}$$

In the lower temperature range, in the limit that $p \ll N_D$ (i.e., the effect of compensation by the donor defects is important), we obtain

$$p = \left(\frac{N_V (N_A - N_D)}{\gamma} \right)^{1/2} e^{-\varepsilon_A / k_B T}. \tag{12}$$

In both cases, we expect a linear dependence of log p on $1/T$, but $U = \varepsilon_A / 2$ or $U = \varepsilon_A$ depending on the temperature range. For the case at hand, where the carrier density ranges from $\approx 10^{17}$ to 10^{19} cm^{-3}, and if $N_A \approx 10^{20}$ cm^{-3} (based on a 1% Cu deficiency), it seems unlikely that the condition $p \ll N_D < N_A$ can be met, so that the donor concentration should be small, and the temperature range should be such that Eq. (11) holds and $\varepsilon_A = 2U \approx 700$ meV, as illustrated in Fig. 8. The Seebeck result is in qualitative agreement, since in this situation, the Fermi level would lie midway between the valence-band maximum and the acceptor defect, in which case $E_F - E_V \approx \varepsilon_A / 2$ and the fit to the data in Fig. 5 yields ε_A in the range 520–700 meV, depending on the exact temperature range used. Using reasonable parameters in Eq. (12) (m_V^* of order the electron mass, γ of order unity) the measured values $N_A \approx 10^{20}$ cm^{-3}, and $\varepsilon_A \approx 0.7$ eV yield $p \approx 10^{18}$ cm^{-3} at room temperature, in agreement with the Hall measurement.

There is evidence in the literature that Cu vacancies are the source of the observed activated *p*-type conductivity. Several theoretical calculations suggest that the Cu-vacancy formation energy is the lowest of likely acceptor defects in Cu_2O and related materials such as $CuAlO_2$ and $SrCu_2O_2$, and that the interstitial oxygen defect, another acceptor, is rather high to be significant.[10,11] Nolan's calculation of the ionization energy of the Cu-vacancy defect in $CuAlO_2$ gives 700 meV.[11] The excellent agreement with our result is perhaps fortuitous, but certainly supports the contention that the activation energy we measure is consistent with ionization of a Cu-vacancy defect. Further, Raebiger *et al.*[10] find that the density of such defects in Cu_2O is likely to be of order 10^{20} cm^{-3}, in order-of-magnitude agreement with our result.

We have no direct spectroscopic evidence of the Cu vacancy, but we can point to some indirect supporting evidence in addition to the agreement between the observed activation energy of the acceptor defect in our samples and the calculated activation energy of the Cu vacancy in $CuAlO_2$. We annealed the $CuAlO_2$ crystal properties in vacuum ($\sim 10^{-3}$ Torr) at 500 °C to remove any interstitial oxygen,

but the annealed samples showed no detectable changes in structure or electrical characteristics, which is in agreement with the report by Lee *et al.*[6] Lee *et al.* also found that $CuAlO_2$ undergoes no change in structural and electrical characteristics when annealed in an oxygen atmosphere at temperatures lower than 900 K; it decomposes when the annealing temperature is higher. Thus we think O interstitials are unlikely.

We also observe small absorption peaks at 1.8 and 0.8 eV (Fig. 6), similar to those at 1.8 and 0.9 eV reported in single-crystal optical absorption measurements on $CuAlO_2$ crystals by Pellicer-Porres *et al.*,[22] who interpret the absorption in terms of transitions between Cu^{2+} *d* levels whose degeneracy is removed by the crystal field, as reported by Ref. 29. To the extent that a Cu-vacancy results in a redistribution of electron density to form a Cu^{2+} species, this interpretation is consistent with ours. The 0.8 eV peak also fits reasonably well with our estimate of 0.7 eV for the binding energy of the acceptor defect level, and may be optical evidence for a valence-band-defect level transition.

A final question is whether the magnetic moment can be identified with the Cu-vacancy defects. Our $CuAlO_2$ crystals have a paramagnetic moment at low temperatures that can be interpreted as resulting from approximately 3×10^{20} cm^{-3} spin-1/2 moments aligning as the thermal energy decreases. As discussed above, this number of defects gives reasonable quantitative agreement with the transport results, since ionization of the defect would produce the required number of carriers. It is also consistent with the approximate Cu-vacancy concentration indicated by EPMA. However, it does not prove that the magnetic signal originates from the carrier-generating defect, and this remains an open question that we only briefly discuss. A Cu vacancy in $CuAlO_2$ results in a deficit of one electron in the O bonds to the Cu. However, O dangling-bond levels are located well below the valence-band maximum in Cu_2O-like materials,[10] so the ground state of the defect is likely to rearrange to give satisfied oxygen bonds, by drawing electron density from the Cu atoms surrounding the vacancy, giving rise to a Cu^{2+} species bound to the vacancy. (Ionizing this species, i.e., drawing electrons from Cu atoms in the bulk, requires thermal activation and results in activated transport.) If the electron spin density is sufficiently localized, then a paramagnetic moment would result. LDA+*U* calculations for the magnetic properties of $Cu_{2-x}O$ by Nolan and Elliot[30] suggest that the electron spin density associated with a vacancy is confined to a region of about 0.6 nm, independent of the size of the supercell used for calculation. The mean spacing of defects at 10^{20} cm^{-3} is approximately 2.2 nm.

V. CONCLUSION

We have reported the structural, optical, transport, and magnetic properties of single crystals of the *p*-type semiconductor $CuAlO_2$ precipitated from a CuO flux. Optical absorption determines that the indirect and direct band gaps are 2.97 and 3.47 eV, respectively. The indirect gap value is larger than most reported from thin-film studies, and in line with other single-crystal studies, indicating that the film re-

ports are likely to be influenced by strain defects. The temperature-dependent transport measurements are reproducible in many samples with low contact resistance. The measurements support a model of band-type conduction in a semiconductor dominated by acceptor defects. The acceptor level, deduced from the carrier-density temperature dependence, is about 700 meV above the valence band. The acceptor defect could be a Cu vacancy, since density-functional calculations suggest that Cu vacancies have the lowest formation energies of all likely acceptor defects and the calculated ionization energy of such a defect, about 700 meV in $CuAlO_2$, is in quantitative agreement with our measurement. The observed paramagnetic moment at low temperature gives a density of 3.4×10^{20} cm^{-3} spin $\frac{1}{2}$ entities. This is consistent with the required number of acceptor defects, so if the Cu vacancies have a localized moment as suggested by some calculations, then the paramagnetism could be from the Cu vacancies, but this remains unresolved. There is a large resistivity anisotropy, with the *ab*-plane resistivity at room temperature about 25 times smaller than that along the *c* axis. In a band-conduction model, this translates to a mobility an-

isotropy, with the Cu planes providing an easier conduction path than the O-Cu-O bonds perpendicular to the planes, though the mechanism for the strong temperature dependence of the mobility is not known. The *ab*-plane and *c*-axis mobilities at 300 K are 3.0 and 0.12 cm^2 V^{-1} s^{-1}, respectively, large enough to support a band-conduction model over a polaron conduction model in this temperature range, at least for the *ab*-plane transport. These relatively large mobilities compared to those reported in polycrystalline bulk or thin-film $CuAlO_2$ also indicate that the properties measured are closer to the intrinsic $CuAlO_2$ properties.

*Corresponding author; tate@physics.oregonstate.edu

†tesl@yonsei.ac.kr

[1] R. Shannon, D. Rogers, and C. Prewitt, Inorg. Chem. **10**, 713 (1971).

[2] N. Duan, M. K. Jayaraj, J. Tate, and A. W. Sleight, Appl. Phys. Lett. **77**, 1325 (2000).

[3] H. Kawazoe, M. Yasukawa, H. Hyodo, M. Kurita, H. Yanagi, and H. Hosono, Nature (London) **389**, 939 (1997).

[4] R. D. Shannon, C. T. Prewitt, and D. B. Rogers, Inorg. Chem. **10**, 719 (1971).

[5] R. D. Shannon, D. B. Rogers, C. T. Prewitt, and J. L. Gillson, Inorg. Chem. **10**, 723 (1971).

[6] M. S. Lee, T. Y. Kim, and D. Kim, Appl. Phys. Lett. **79**, 2028 (2001).

[7] K. Koumoto, H. Koduka, and W.-S. Seo, J. Mater. Chem. **11**, 251 (2001).

[8] H. Yanagi, S. Inoue, K. Ueda, H. Kawazoe, H. Hosono, and N. Hamada, J. Appl. Phys. **88**, 4159 (2000).

[9] B. J. Ingram, T. O. Mason, R. Asahi, K. T. Park, and A. J. Freeman, Phys. Rev. B **64**, 155114 (2001).

[10] H. Raebiger, S. Lany, and A. Zunger, Phys. Rev. B **76**, 045209 (2007).

[11] M. Nolan, Thin Solid Films **516**, 8130 (2008).

[12] B. Ingram, G. Gonzalez, and T. Mason, Chem. Mater. **16**, 5616 (2004).

[13] T. Ishiguro, A. Kitazawa, N. Mizutani, and M. Kato, J. Solid State Chem. **40**, 170 (1981).

[14] H. Gong, Y. Wang, and Y. Luo, Appl. Phys. Lett. **76**, 3959 (2000).

[15] F. A. Benko and F. P. Koffyberg, J. Phys. Chem. Solids **45**, 57 (1984).

[16] W. Lan, M. Zhang, G. Dong, Y. Wang, and H. Yan, J. Mater. Res. **22**, 3338 (2007).

[17] K. Seeger, *Semiconductor Physics: An Introduction* (Springer, Berlin, 1982).

[18] E. C. Jones, D. P. Norton, D. K. Christen, and D. H. Lowndes, Phys. Rev. Lett. **73**, 166 (1994).

[19] J. Pellicer-Porres, D. Martínez-García, A. Segura, P. Rodríguez-Hernández, A. Muñoz, J. C. Chervin, N. Garro, and D. Kim, Phys. Rev. B **74**, 184301 (2006).

[20] M. K. Singh, S. Dussan, G. L. Sharma, and R. S. Katiyar, J. Appl. Phys. **104**, 113503 (2008).

[21] N. F. Mott, *Conduction in Non-Crystalline Materials* (Oxford University Press, New York, 1956).

[22] J. Pellicer-Porres, A. Segura, A. S. Gilliland, A. Muñoz, P. Rodríguez-Hernández, D. Kim, M. S. Lee, and T. Y. Kim, Appl. Phys. Lett. **88**, 181904 (2006).

[23] C. Kittel, *Introduction to Solid State Physics* (Wiley, New York, 1986).

[24] R. W. Selwood, *Magnetochemistry* (Interscience, New York, 1956).

[25] B. X. Yang, T. R. Thurston, J. M. Tranquada, and G. Shirane, Phys. Rev. B **39**, 4343 (1989).

[26] M. O'keeffe and F. S. Stone, J. Phys. Chem. Solids **23**, 261 (1962).

[27] C. B. Azzoni, A. Paeleari, and G. B. Parravicini, J. Phys.: Condens. Matter **4**, 1359 (1992).

[28] J. S. Blackmore, *Semiconductor Statistics* (Pergamon, Oxford, 1962).

[29] V. B. Kapustianik, V. V. Bazhan, and Yu. M. Korchak, Phys. Status Solidi B **234**, 674-688 (2002).

[30] M. Nolan and S. D. Elliot, Phys. Chem. Chem. Phys. **8**, 5350 (2006).